Automatic detection of A phases of the Cyclic Alternating Pattern during sleep

Sara Mariani, *Member, IEEE,* Anna M. Bianchi, *Member, IEEE,* Elena Manfredini, Valentina Rosso, Martin O. Mendez, Liborio Parrino, Matteo Matteucci, Andrea Grassi, Sergio Cerutti, *Fellow, IEEE,* and Mario G. Terzano

Abstract— **This study aimed to develop an automatic algorithm to detect the activation phases (A phases) of the Cyclic Alternating Pattern. The sleep EEG microstructure of 4 adult, healthy subjects was scored by a sleep medicine expert. Features were calculated from each of the six EEG bands (low delta, high delta, theta, alpha, sigma and beta), and three additional characteristics were computed: the Hjorth activity in the low delta and high delta bands, and the differential variance of the raw EEG signal. The correlation between couples of features was analyzed to find redundancies for the automatic analysis. The features were used to train an Artificial Neural Network to automatically find the A phases of CAP. The data were divided into training, validation and testing set, and the visual scoring provided by the clinician was used as the desired output. The statistics on the second by second classification show an average sensitivity equal to 76%, specificity equal to 83% and accuracy equal to 82%. The results obtained are encouraging, since an automatic classification of the A phases could benefit the practice in clinics, preventing the physician from the time-consuming activity of visually scoring the sleep microstructure over the whole eight-hour sleep recordings. Moreover, it would provide an objective criterion capable of overcoming the problems of inter-scorer variability.**

I. INTRODUCTION

CYCLIC Alternating Pattern (CAP) is a periodic activity on the EEG signal that occurs during non-REM (NREM) sleep. CAP is composed of sequences of transient electrocortical events (phase A) that are distinct from the background (phase B), as shown in Fig. 1. The organization of A and B phases of CAP defines the microstructure of sleep.

Both phase A and phase B recur at intervals up to 1 minute long. Each phase A is characterized by

S. Mariani, E. Manfredini, A. M. Bianchi and S. Cerutti are with Politecnico di Milano, Dept. of Biomedical Engineering, P.zza Leonardo da Vinci 32, 20133, Milan, Italy (tel: +390223999503, e-mail: sara1.mariani@mail.polimi.it, elena.manfredini@mail.polimi.it, annamaria.bianchi@polimi.it, cerutti@biomed.polimi.it).

M. Matteucci is with Politecnico di Milano, Dept. of Information Engineering, P.zza Leonardo da Vinci 32, 20133, Milan, Italy (e-mail: matteucc@elet.polimi.it

V. Rosso, A. Grassi, L. Parrino and M. G. Terzano are with the Sleep Disorders Center of "Ospedale Maggiore di Parma", via Gramsci 14, 43126, Parma, Italy (e-mail: vrosso@ao.pr.it, andrea.grassi@studenti.unipr.it, liborio.parrino@unipr.it, mterzano@unipr.it).

M. O. Mendez is with Facultad de Ciencias, Diagonal Sur S/N, Zona Universitaria, San Luis Potosi, S.L.P., Mexico (e-mail: mmendez@galia.fc.uaslp.mx).
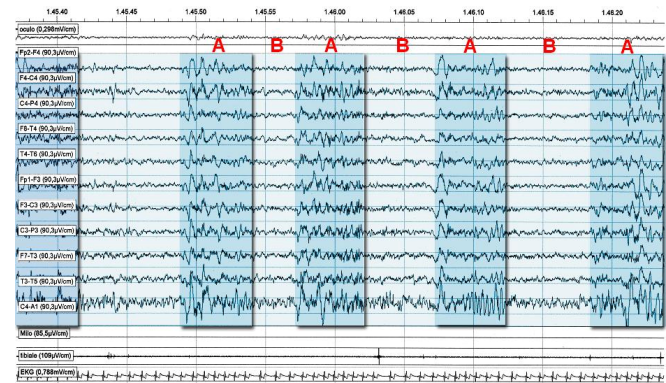
Fig. 1: An example of Cyclic Alternating Pattern in sleep stage 2. The boxes outline the phases A of CAP.

frequency/amplitude components which underline transient brain activation and can be classified into three subtypes: A1 are characterized by strong delta waves (0.5-4 Hz); A2 have rapid activities that occur for 20-50% of the total activation time; A3 are characterized by rapid activities, especially beta (15-30 Hz), that occupy more than the 50% of the total time [1]. A phase A, and the following phase B, shape a CAP cycle and at least two consecutive CAP cycles define a CAP sequence.

CAP sleep contains relevant information for evaluating the sleep quality of a subject. The ratio between NREM CAP sleep and total NREM sleep, called *CAP-rate*, and the distribution of CAP through the sleep stages are used to better characterize sleep pathologies such as nocturnal frontal lobe epilepsy, sleep apnea and insomnia [2]. Nowadays, the CAP evaluation is a time-consuming task, since neurologists in sleep centers have to analyze visually the EEG of whole night sleep recordings. Moreover, it has been estimated that the average inter-scorer agreement between the classifications of single EEG trace by two different clinicians ranges from 69 to 77% [3].

In order to solve these problems, some studies have implemented automatic detection methods of CAP A-phases. Among them, we report [4]-[9]. In all these methods, the computation of "band descriptors", performed in combination with the superimposition of thresholds and logic criteria, has allowed the achievement of good results. However, further effort has to be put into the research for new features to create a robust automatic method, before it can be effectively introduced in everyday clinics.

The present study attempts to automatically recognize, from the EEG signal, the activations that build up the sleep microstructure. This system could reduce the needed time for scoring the activations and would also damp the inter-scorer variability.

II. MATERIALS AND METHODS

The sleep EEG recordings of 4 healthy adult subjects were studied. The subjects did not present any primary medical or psychiatric disorder and used no drugs affecting the central nervous system. The recordings were provided by the Sleep Center from the "Ospedale Maggiore di Parma". The polygraphic recordings lasted around 8 hours each, and included several Electroencephalographic (EEG) derivations, Electromyogram and Electrocardiogram. Each signal was acquired and scored by an expert clinician on the commercial software Somnologica Studio (Embla Systems[TM]).

The expert visually scored the following events:
- macrostructure: sleep stages 1-4, wake, REM sleep, movement time
- microstructure: A phases

C3-A2 or C4-A1 leads were equivalently used for the data analysis. The data were exported from Somnologica to the programming environment Matlab (The Mathworks Inc.) at a sampling frequency equal to 100 Hz.

A. Creation of the descriptors

The signal segments belonging to wake and REM sleep were removed, and only NREM sleep was analyzed. The EEG signal was filtered with a low-pass anti-aliasing filter at 30 Hz. Then, it was separated in the following bands: Low Delta (0.5 Hz - 2 Hz), High Delta (2 Hz – 4 Hz), Theta (4 Hz - 8 Hz), Alpha (8 Hz - 12 Hz), Sigma (12 Hz - 15 Hz), and Beta (15 Hz - 30 Hz). A FIR filter with 30 coefficients and a Kaiser window was used for this purpose. For each band, the resulting signal was squared and normalized between 0 and 1 (with respect to the maximum power in the band), and, for each of the six bands in exam, band descriptors were implemented:

$$d_b(t) = \frac{p_s - p_l}{p_l} \qquad (1)$$

where d_b is the power in the considered band b at a certain second, and p_s and p_l are the mean power in the considered band on a window of 2 and 64 seconds, respectively. The windows were chosen according to previous studies [5], [6]. After the computation of the band descriptors, some outlier values remained, due to electrical or movement artifact. They were removed by setting to zero all the values that exceeded the experimentally determined threshold of 10σ, where σ is the descriptor standard deviation. The descriptors were normalized again between 0 and 1 with respect to their maximum value and eventually subsampled at 1 Hz by averaging on non-overlapping windows of 1 s each.

A further descriptor was created using the Hjorth parameters [10] applied to the high delta and to the low delta bands. The first parameter is called *activity* and it is the variance σ of the signal segment. The activity of the signal filtered in the low delta and high delta bands was calculated over 3-second windows, centered on the second of interest. These descriptors are meant to capture the overall increase of the delta power occurring during the activations over a longer time span, in order to avoid misclassification due to spurious peaks in the low delta and high delta descriptors not belonging to activations.
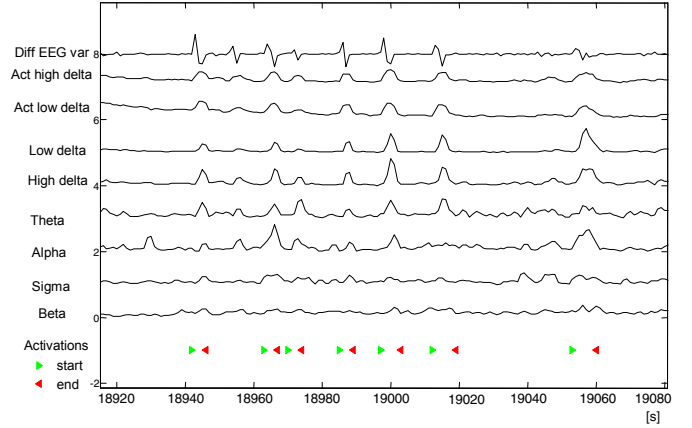

Fig. 2: Behavior of the descriptors in correspondence of the visually scored A phases.

Finally, the variance of the raw EEG signal was taken into account as a new feature for the distinction of CAP A phases. Outliers were eliminated from the raw EEG signal with the same process used for the computation of the band descriptors and the variance was computed on windows of 1 second. The variance difference between one 1-second window and the previous one was calculated and the result normalized by its maximum value. An example of the trend of the descriptors in correspondence of the visually-scored activations in sleep stage 2 is shown in Fig. 2. It can be noticed that the descriptors in the low frequency bands and the activity descriptors show evident peaks in correspondence of the visually scored activations, the other band descriptors have a certain, although less clear, variation during the activations, and the differential variance of the EEG has positive peaks where the activations start and negative peaks where they end.

B. Correlation analysis

In order to eliminate redundancies prior to the detection step, a correlation analysis among the descriptors listed above was performed. For every couple of descriptors, the Pearson's product-moment correlation coefficient was computed:

$$\rho_{X,Y} = \frac{cov(X,Y)}{\sigma_X \sigma_Y} = \frac{E[(X - \mu_X)(Y - \mu_Y)]}{\sigma_X \sigma_Y} \qquad (2)$$

where X and Y were the two descriptors in exam, μ_X and μ_Y their mean values, and σ_X and σ_Y their standard deviations. The correlation coefficients are reported in Table I.

The descriptors mostly contain complementary information, as can be inferred from the correlation coefficients, which are, in general, indicative of a moderate or low linear dependence. The only exceptions are represented by the low delta and high delta descriptors, having a correlation coefficient equal to 0.86, and by the low delta and high delta Hjorth activity descriptors, having a correlation coefficient equal to 0.94. Therefore, in the light of an automatic classification, to avoid redundancies and lighten the computational burden, the low delta descriptor and the low delta activity can be eliminated in favor of those in the high delta band, containing similar information.

	Low δ	High δ	θ	α	σ	β	Low δ act	High δ act	Var
Low δ	1	0.86	0.61	0.39	0.31	0.30	0.50	0.46	0.28
High δ		1	0.74	0.43	0.33	0.31	0.48	0.52	0.30
θ			1	0.54	0.38	0.38	0.36	0.41	0.23
α				1	0.49	0.52	0.21	0.21	0.14
σ					1	0.65	0.22	0.21	0.13
β						1	0.15	0.11	0.11
Low δ act							1	0.94	0.59
High δ act								1	0.57
Var									1

Due to its symmetry, only half of the table is shown. The greek letters indicate the frequency bands of the EEG.

C. Automatic detection: Implementation of the Neural Network

Before implementing the neural network, two preprocessing steps were carried out:
1) In order to homogenize the values of the descriptors around the activations, a moving window *f(x)* was applied to all the band descriptors besides the delta, and to the activity descriptor in the high delta band:

$$x_t = argmax_{x \in [x_t - b, x_t + b]} f(x) \quad (3)$$

where x_t is the center of the window, and b is equal to 2 for the band descriptors and to 1 for the activity.
For the differential variance of the EEG, the absolute value was computed.
2) In order to avoid a bias in the classifier, we used an equal number of samples for each of the two classes (1=activation, 0=non-activation).

Based on the results from sections *A* and *B*, a three-layer supervised network was chosen, with a 7-neuron input layer, a *n*-neuron hidden layer, and a 2-neuron output layer. The number *n* of the hidden layer neurons varied from 2 to 30. The chosen activation function for the hidden and the output layers was *logsig*. The training mode was the backpropagation with the Levenberg-Marquardt algorithm. A schematic structure of the network is represented in Fig. 3.

In order to obtain a network with good generalization capability, the Leave One Out technique was exploited: for each subject to be classified, several neural networks were trained using the remaining three subjects' recordings. The data of one of the three subjects at the time were used as the *testing set* (approximately 30,000 samples), whereas the remaining data of two subjects (approximately 90,000 samples) were equally divided into *training set* and *validation set*.

With these data, and for each value of *n*, 2<*n*<30, the neural networks were trained and restarted 10 times, and the one with the best performance (the least training error) was chosen, in order to avoid local minima problems. The network with the best performance was then chosen among those obtained with different values of *n*. The optimal values for *n* ranged from 14 to 21, depending on the fold. This *modus operandi* led to 3 "optimal" neural networks for each of the four subjects. The three networks were then applied to
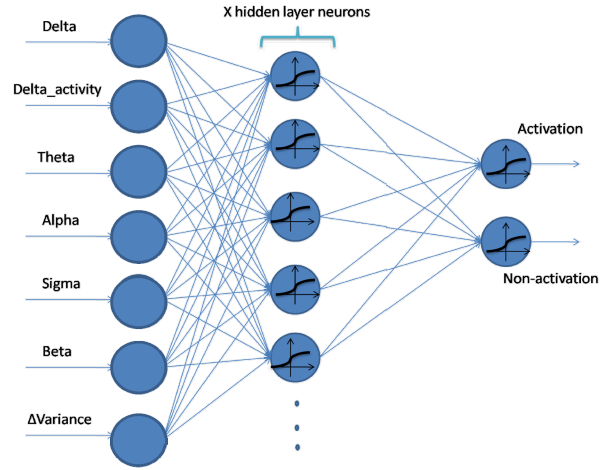

Fig. 3: Structure of the Neural Network.

Fig. 4: Scheme of the post-processing procedure.

the corresponding subject's data, in order to obtain three different classifications for each sample. The final classification was computed as the rounded mean value of the three network outputs.

Since A phases cannot last more than 60 seconds or less than 2 seconds [1], the automatically recognized activations lasting longer than 60 s were divided by a 2-neuron-competitive neural network for clustering. The k-means algorithm for clustering was alternatively implemented, but it was rejected because of its poorer performance, the discussion of which goes beyond the purpose of this paper.

Furthermore, a post-processing was applied to eliminate automatically detected phases A or phases B shorter than 2 seconds, as shown in Fig. 4.

III. RESULTS

Sensitivity, specificity, and accuracy, calculated through a second-by-second comparison of the automatic classification vectors with the visual classification vectors, are reported in Table II. It can be noticed that the average accuracy is very high, equal to 81.55%.

The 4-minutes screenshot in Fig. 5 shows an example of the result of the automatic classification: the solid boxes highlight the correct scorings, the dashed boxes cases where a visually-scored A phase was considered as two separate A phases by the automatic classifier, the dotted boxes highlight cases of correctly recognized activations with different durations in the visual and the automatic case.

TABLE II

STATISTICS OBTAINED FOR THE AUTOMATIC CLASSIFICATION OF THE A PHASES WITH THE ARTIFICIAL NEURAL NETWORK

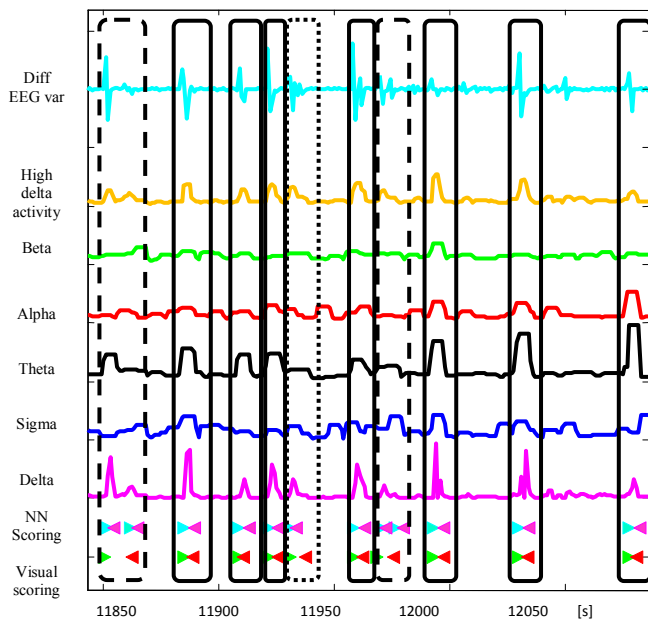| Subject	Sensitivity (%)	Specificity (%)	Accuracy (%)
1	67.6	88.4	84.2
2	77.7	79.9	79.6
3	80.9	75.0	75.6
4	76.4	88.9	86.8
Mean	**75.65**	**83.05**	**81.55**

Fig. 5: Classification results obtained with the neural network.

It can be seen how the recognition performed by the automatic classifier has a very high accuracy, and is faithful to the trend of the descriptors, detecting all their peaks.

IV. DISCUSSION AND CONCLUSION

This study presented a novel algorithm for the classification of sleep microstructure, based on the identification of distinctive features of the EEG and exploiting an Artificial Neural Network. Our main observations are:

1. The sleep microstructure could be automatically detected using a single EEG lead
2. This method is entirely automatic, without any need of human intervention
3. With a limited number of descriptors, a complete frame of the EEG variations that occur during CAP A phases could be captured
4. The Neural Network seems to be a robust machine-learning tool to classify the sleep microstructure events.

The use of a single EEG trace makes the algorithm simple to hand and enlightens the computational burden of the method: the introduction of a second trace, perhaps a frontal derivation, where the delta components are more represented, could somehow improve the classification at the expense of the computational load.

Out of the automatic methods used to detect the sleep microstructure, some published methods need the clinician intervention [9], obtaining moderate classification results and reducing the time for the detection of the microstructure. However, the advantage of the current method is the total independence from any *a priori* information besides the mere REM/NREM distinction.

The introduction of new features, other than the band descriptors, improves the classification: the Hjorth activity descriptor is able to better account for the average increase of delta power during activations, whereas the differential variance of the raw EEG signal captures the abrupt

frequency variations happening during CAP A phases.

Due to the complexity of the data, a non-linear, inductive machine-learning method like a Neural Network constitutes a much more accurate classifier than a simple threshold method. Moreover, differently from previous studies [5], [6], [8], that also report high accuracy values, ranging around 77-84%, here the statistics were computed not only by applying a mere overlap criterion between visually and automatically scored activations, but considering each 1-second window as an observation, leading to a much more precise statistic.

In spite of the limited amount of subjects, the statistics obtained are encouraging, and suggest that better results could be obtained increasing the dimensions of the dataset and thus the size of the training set for the network.

The intrinsic characteristics of the method, based on a 1-second moving window, increase the potential discrepancy between visual and automatic definition of phase A duration. In order to overcome this problem, before identifying the CAP, we suggest having an expert perform an *a posteriori* validation and control of the duration of each potential A phase as scored by the automatic algorithm. Further classifiers could be introduced based on different techniques, such as Support Vector Machines, or on different parameters, such as fractal or entropy measures.

In conclusion, the algorithm here presented has an accuracy that is comparable with the inter-scorer agreement values reported in literature [3]. Such a method would not only allow an *objective* microstructure scoring, but would also highly speed up the study of the sleep microstructure in everyday clinic practice and research.

REFERENCES

[1]   M. G. Terzano, L. Parrino, A. Sherieri, R. Chervin, S. Chokroverty, C. Guilleminault, M. Hirshkowitz, M. Mahowald, H. Moldofsky, A. Rosa, R. Thomas and A. Walters, "Atlas, rules, and recording techniques for the scoring of cyclic alternating pattern (CAP) in human sleep," *Sleep Med.,* vol. 2, pp. 537-553, 2001.

[2]   P. Halász, M. Terzano, L. Parrino and R. Bódizs, "The nature of arousal in sleep," *J. Sleep Res.,* vol. 13, pp. 1-23, 2004.

[3]   A. Rosa, G. R. Alves, M. Brito, M. C. Lopes and S. Tufik, "Visual and automatic cyclic alternating pattern (CAP) scoring: Inter-rater reliability study," *Arq. Neuropsiquiatr.,* vol. 64, 2006.

[4]   A. C. Rosa, L. Parrino and M. G. Terzano, "Automatic detection of cyclic alternating pattern (CAP) sequences in sleep: Preliminary results," *Clinical Neurophysiology,* vol. 110, pp. 585-592, 1999.

[5]   C. Navona, U. Barcaro, E. Bonanni, F. Di Martino, M. Maestri and L. Murri, "An automatic method for the recognition and classification of the A-phases of the cyclic alternating pattern," *Clinical Neurophysiology,* vol. 113, pp. 1826-1831, 2002.

[6]   U. Barcaro, E. Bonanni, M. Maestri, L. Murri, L. Parrino and M. G. Terzano, "A general automatic method for the analysis of NREM sleep microstructure," *Sleep Med.,* vol. 5, pp. 567-576, 2004.

[7]   F. De Carli, L. Nobili, M. Beelke, T. Watanabe, A. Smerieri, L. Parrino, M. G. Terzano and F. Ferrillo, "Quantitative analysis of sleep EEG microstructure in the time-frequency domain," *Brain Res. Bull.,* vol. 63, pp. 399-405, 2004.

[8]   R. Largo, C. Munteanu and A. Rosa, "CAP event detection by wavelets and GA tuning," in 2005, pp. 44-48.

[9]   R. Ferri, O. Bruni, S. Miano, A. Smerieri, K. Spruyt and M. G. Terzano, "Inter-rater reliability of sleep cyclic alternating pattern (CAP) scoring and validation of a new computer-assisted CAP scoring method," *Clinical Neurophysiology,* vol. 116, pp. 696-707, 2005.

[10] B. Hjorth, "EEG analysis based on time domain properties," *Electroencephalography & Clinical Neurophysiology,* vol. 29, pp. 306-310, 1970.